

The $U(1)$ Problem in Chiral Random Matrix Models

Romuald A. Janik¹, Maciej A. Nowak², Gábor Papp³, and Ismail Zahed⁴

¹ Department of Physics, Jagellonian University, 30-059 Krakow, Poland

² GSI, Plankstr.1, D-64291 Darmstadt & Institut für Kernphysik, TH Darmstadt, Germany & Department of Physics, Jagellonian University, 30-059 Krakow, Poland;

³ GSI, Plankstr. 1, D-64291 Darmstadt, Germany &

Institute for Theoretical Physics, Eötvös University, Budapest, Hungary

⁴ Department of Physics, SUNY, Stony Brook, New York 11794, USA.

(February 1, 2008)

We show that conventional asymmetric chiral random matrix models (ChRMM), with a gaussian distribution in the asymmetry, provide for a screening of the topological charge and a resolution of the $U(1)$ problem in the unquenched approximation. Our exact results to order $1/N$ are in agreement with numerical estimates using large ensembles of asymmetric ChRMM with gaussian distributions.

I. INTRODUCTION

In QCD the axial $U(1)$ symmetry is not apparent in the spectrum, although a non-vanishing quark condensate suggests the existence of a ninth Goldstone boson. This is the $U(1)$ problem. The resolution of this apparent problem is believed to follow from the chiral anomaly [1]. 't Hooft has suggested a specific mechanism using instantons [2]. Witten has proposed a resolution in the context of the large N_c (number of colors) limit [3], an idea that was interpreted by Veneziano in terms of vector ghosts [4].

In all existing scenarios for the resolution of the $U(1)$ problem, it is crucial that the topological susceptibility is nonzero in both the quenched and unquenched (with massive quarks) approximation. Lattice simulations appear to support this assumption both for quenched [5] and unquenched [6], although the idea may be at odd with translational invariance and current identities [7]. This notwithstanding, it was argued by few that a statistical ensemble of topological charges may yield to the screening of the bare topological susceptibility and the resolution of the $U(1)$ problem [8]. This scenario will be considered in the context of standard ChRMM [9–12].

Standard ChRMM follow from the constant mode sector of the instanton liquid model [13–15], regarded as a statistical ensemble of topological zero modes. As models, they offer a minimal framework for discussing the interplay between (chiral) symmetry, typical scales and the thermodynamical limit. In these models gaussian randomness is enough to cause the spontaneous breaking of chiral symmetry (hermitean matrices) or the spontaneous breaking of holomorphic symmetry (nonhermitean

matrices) in the thermodynamical limit. They have also been used to investigate issues related to the universality of “noise-fluctuations” in Dirac spectra both in the microscopic [9] and macroscopic [16] limit.

In so far, most of the analyses carried in the context of standard ChRMM have been conducted using standard and symmetric ChRMM. In the context of the instanton liquid model this means that the number of instantons and the number of antiinstantons is fixed. In this case there is no resolution of the $U(1)$ problem. In this letter, we will consider a statistical ensemble of asymmetric ChRMM with a gaussian distribution for the asymmetry. The physical motivation for this model stems from the coarse grained version of the instanton liquid model [19]. In section 2, we will discuss basic QCD Ward identities emphasizing the role of a non-vanishing topological susceptibility in the resolution of the $U(1)$ problem. In section 3, we streamline the phenomenological arguments for standard but asymmetric ChRMM with a gaussian distribution for the matrix asymmetry. In section 4, we use a diagrammatic analysis based on a $1/N$ expansion to solve the $U(1)$ problem. Our analytical results for the unquenched topological, scalar and pseudoscalar susceptibilities are in agreement with numerical estimates using large asymmetric matrices. Our conclusions are in section 5. We elaborate on some derivations in the Appendices. Throughout, we will use four-dimensional arguments in Minkowski space. The transcription to ChRMM will be done through their Euclidean four-dimensional analogue.

II. QCD WARD IDENTITY

The topological term in the QCD Lagrangian $\theta \Xi$ is a total divergence

$$\Xi = \frac{g^2}{32\pi^2} G_{\mu\nu}^a \tilde{G}^{\mu\nu a} = \partial^\mu K_\mu \quad (1)$$

where K_μ is the Loos-Chern-Simons current. For N_f flavors of quarks with current masses m_f , the gauge-invariant flavor axial-singlet current $j_{\mu 5}^{\text{inv}}$ is anomalous,

$$\partial^\mu j_{\mu 5}^{\text{inv}} = 2N_f \Xi + 2 \sum_f^{N_f} m_f \bar{\psi}_f i\gamma_5 \psi_f \quad (2)$$

In a θ state, the expectation value of (2) implies

$$0 = 2N_f \langle \theta | \Xi | \theta \rangle + 2 \sum_f^{N_f} \langle \theta | m_f \bar{\psi}_f i \gamma_5 \psi_f | \theta \rangle \quad (3)$$

by translational invariance. In particular, the topological susceptibility $\chi(\theta)$ is given by

$$\chi(\theta) = \frac{\partial \langle \theta | \Xi | \theta \rangle}{\partial \theta} = -\frac{1}{N_f} \sum_f^{N_f} \frac{\partial}{\partial \theta} \langle \theta | m_f \bar{\psi}_f i \gamma_5 \psi_f | \theta \rangle \quad (4)$$

The absence of a physical massless $U(1)$ boson for quarks of equal masses $m_f = m$, gives [7]

$$\begin{aligned} 0 &= \int d^4x \partial^\mu \langle \theta | T^* j_{\mu 5}^{\text{inv}}(x) \bar{\psi} i \gamma_5 \psi(0) | \theta \rangle \\ &= -2i \langle \theta | \bar{\psi} \psi | \theta \rangle - 2i \frac{N_f^2}{m} \chi(\theta) \\ &\quad + 2m \int d^4x \langle \theta | T^* \bar{\psi} i \gamma_5 \psi(x) \bar{\psi} i \gamma_5 \psi(0) | \theta \rangle \end{aligned} \quad (5)$$

where we have made use of (3,4). T^* is the covariantized T-product. For $\theta = 0$, it follows from (5) that

$$i\chi_{top} = -\frac{im}{N_f^2} \langle \bar{\psi} \psi \rangle + \frac{m^2}{N_f^2} \int d^4x \langle T^* \bar{\psi} i \gamma_5 \psi(x) \bar{\psi} i \gamma_5 \psi(0) \rangle \quad (6)$$

where we have set $\chi_{top} = \chi(0)$, in agreement with earlier results [17,18]. The resolution of the $U(1)$ problem stems from the observation that for small m , the absence of a $U(1)$ Goldstone mode requires that $\chi_{top} = -m \langle \bar{\psi} \psi \rangle / N_f^2$ to order $\mathcal{O}(m^2)$.

A rerun of the above argument for the $SU(N_f)$ currents and densities yields the flavor non-singlet relation

$$\begin{aligned} 0 &= -\frac{i}{2} \langle \bar{\psi} [\lambda_I, \lambda_J]_+ \psi \rangle \\ &\quad + m \int d^4x \langle T^* \bar{\psi} i \gamma_5 \lambda_I \psi(x) \bar{\psi} i \gamma_5 \lambda_J \psi(0) \rangle \end{aligned} \quad (7)$$

which shows that for small m there should be a multiplet of $N_f^2 - 1$ Goldstone modes. Contrasting (6) with (7) shows the importance of a non-vanishing topological susceptibility in the resolution of the $U(1)$ problem. It was originally argued by Witten [3] that further consistency with large N_c arguments requires that the quenched topological susceptibility χ_* be nonzero as well. Current lattice simulations seem to support this conjecture [5], although there may be subtleties as we indicated above [7].

III. CHRMM

A number of effective models aimed at describing the long wavelength physics of the QCD vacuum including

the $U(1)$ anomaly, have been put forward by several authors [20]. In these effective models it is important that point-like pseudoscalars are coupled to point-like glueballs to achieve consistency with the QCD anomalies (axial and scale anomaly).

Such effective models arise naturally from microscopic descriptions of the QCD vacuum using a random ensemble of instantons and antiinstantons [13–15]. In the “coarse grained instanton model” [15,19], the effective “glueball” fields are identified with

$$\frac{g^2}{32\pi^2} G \cdot G(x) \rightarrow (n_+ + n_-)(x) \quad (8)$$

$$\frac{g^2}{32\pi^2} G \cdot \tilde{G}(x) \rightarrow (n_+ - n_-)(x) \quad (9)$$

where $n_\pm(x)$ is the density of instantons (+) and antiinstantons (-). The $U(1)$ anomaly is saturated by assuming that the distribution in the number difference $(n_+ - n_-)$ (susceptibility of the quenched vacuum) is gaussian. The scale anomaly is also saturated by assuming that the distribution in the number density $(n_+ + n_-)$ (compressibility of the quenched vacuum) follows from a logarithmic ensemble [19,20].

A. Symmetric ChRMM

Standard ChRMM are schematic versions of current descriptions of the instanton liquid model [13–15]. One essentially truncates the QCD partition function to the space of instanton-antiinstanton zero modes and furthermore assumes that the fermionic overlaps are randomly distributed with a Gaussian measure. Specifically

$$Z = \left\langle \det^{N_f} \mathbf{Q} \right\rangle_A \quad (10)$$

where

$$\mathbf{Q} = \begin{pmatrix} im_f & A^\dagger \\ A & im_f \end{pmatrix} \quad (11)$$

and A is an $N \times N$ matrix distributed with a weight

$$P(A) = e^{-N \Sigma \text{tr} A A^\dagger} \quad (12)$$

where Σ is a fixed scale related to the quark condensate through $\langle \psi^\dagger \psi \rangle = 1/\pi \Sigma$. For simplicity $\Sigma = 1$ in the arguments to follow. The large N limit is directly linked to the thermodynamic limit through the choice $N/V_4 = 1$. In other words the number of zero modes is made commensurate to the four volume V_4 , to insure a non-vanishing chiral condensate in the thermodynamical limit.

One can easily check that for such ensembles, the topological susceptibility is zero. This is due to the fact that in (10) we have used symmetric matrices, *i.e.* in the instanton liquid model, we have set the number of instantons equal to the number of antiinstantons.

B. Asymmetric ChRMM

The above constraint can be relaxed following [19,21,22] through

$$Z = \sum_{n_\pm}^* Z_{n_+, n_-} e^{-\frac{\chi^2}{2N\chi_*}} \quad (13)$$

where $\chi = n_+ - n_-$ is the difference between the number of instantons and antiinstantons and Z_{n_+, n_-} is as before (10), but with the A 's now rectangular and $n_+ \times n_-$ complex valued. The star in (13) indicates that the sum is restricted to $n_+ + n_- = 2N$ with N eventually going to infinity. The issue related to the scale anomaly [23] (for our case an unrestricted sum in (13)) will be discussed elsewhere. The topological susceptibility in the limit of infinite quark mass (quenched) is in this case just

$$\chi_{top} = \frac{1}{N} \langle \chi \chi \rangle = \chi_* \quad (14)$$

Although (13) describes a statistical ensemble of point-like topological defects, that is zero correlation length, the latters are spread over a gaussian of width $\sqrt{N}\chi_*$, resulting into a finite correlation length or topological susceptibility in the thermodynamical limit. In the next section we evaluate the pseudoscalar and topological susceptibilities for the ensemble (13) in the context of a $1/N$ expansion.

IV. $U(1)$ PROBLEM IN CHRMM

A measure of the axial-singlet charge in the QCD vacuum in the presence of light quarks is given by the pseudoscalar axial-singlet susceptibility

$$\chi_{ps} = \frac{1}{V_4} \int d^4x \langle T^* \bar{\psi} \gamma_5 \psi(x) \bar{\psi} \gamma_5 \psi(0) \rangle \quad (15)$$

A resolution of the $U(1)$ problem requires that χ_{ps} remains finite as $V_4 \rightarrow \infty$ followed by $m \rightarrow 0$.

To help investigate (15) in the context of standard ChRMM, we recast (13) in the form of a partition function over Grassmann variables

$$Z = \sum_{n_\pm}^* \int d\psi^\dagger d\psi dA e^{-\sum_{N_f} \psi^\dagger \mathbf{Q} \psi - N \text{tr} A A^\dagger - \chi^2 / 2N\chi_*} \quad (16)$$

The Euclidean analogue of (15) in ChRMM is

$$\begin{aligned} \chi_{ps} &= \frac{1}{N} [-\langle \text{tr} \mathbf{Q}^{-1} \gamma_5 \mathbf{Q}^{-1} \gamma_5 \rangle] \\ &+ \frac{1}{N} [\langle \text{tr} (\mathbf{Q}^{-1} \gamma_5) \text{tr} (\mathbf{Q}^{-1} \gamma_5) \rangle_c] \end{aligned} \quad (17)$$

where all averages are carried using (16) that is (13). A naive expectation based upon large N counting rules suggests that the second term in (17) is subleading in the thermodynamic limit. As we will show below, this expectation is not born out by calculations.

A. The Rules and Resolvent

• Feynman Rules

To assess (17) we use a $1/N$ expansion. The Feynman rules associated to (15) are shown in Fig. 1. The bare quark propagator is $1/(-im)$ and the bare gluon propagator is

$$\begin{aligned} \mathcal{D} = \langle A_b^a A_d^c \rangle &= \left[\frac{1}{N} \begin{pmatrix} 1 & 0 \\ 0 & 0 \end{pmatrix}_{ad} \otimes \begin{pmatrix} 0 & 0 \\ 0 & 1 \end{pmatrix}_{bc} \right. \\ &\quad \left. + \frac{1}{N} \begin{pmatrix} 0 & 0 \\ 0 & 1 \end{pmatrix}_{ad} \otimes \begin{pmatrix} 1 & 0 \\ 0 & 0 \end{pmatrix}_{bc} \right] \otimes \mathcal{F} \end{aligned} \quad (18)$$

Here a, b, c and d run from 1 to $2N$, \otimes denotes tensor product and \mathcal{F} is a flavor bearing matrix with flavor indices f_i . For $N_f = 3$

$$\mathcal{F}_{f_2 f_4}^{f_1 f_3} = \delta_{f_4}^{f_1} \delta_{f_3}^{f_2} = \frac{1}{2} ([\lambda_0]_{f_2}^{f_1} [\lambda_0]_{f_4}^{f_3} + [\lambda_I]_{f_2}^{f_1} [\lambda_I]_{f_4}^{f_3}) \quad (19)$$

following a standard decomposition. In terms of (19), the bare gluon propagator may be rewritten in the form

$$\mathcal{D} = \frac{1}{4N} ((\mathbf{1} \lambda_I) \otimes (\mathbf{1} \lambda_I) - (\gamma_5 \lambda_I) \otimes (\gamma_5 \lambda_I)) \quad (20)$$

with I running from 0 to 8. We use the normalization $\text{tr} \lambda_I \lambda_J = 2\delta_{IJ}$. The flavor decomposition stemming from (20) is reminiscent of the flavor interaction in a schematic quark-meson effective theory of the Nambu-Jona-Lasinio type.

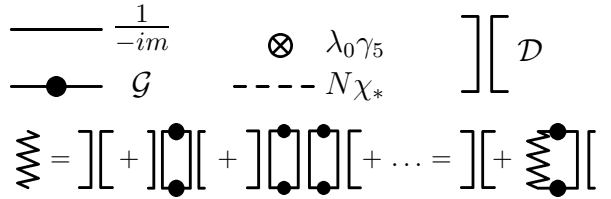


FIG. 1. Feynman rules. In the upper part: the bare quark propagator $1/(-im)$, the dressed one (\mathcal{G}), the γ_5 vertex, the bare χ propagator and the bare gluon propagator \mathcal{D} . In the lower part the dressing of the gluon propagator is shown, the last equality representing the Schwinger-Dyson equation.

• Resolvent

For a single flavor we define the resolvent

$$\mathcal{G}(z) = \frac{1}{2N} \left\langle \frac{1}{z - \begin{pmatrix} im & A^\dagger \\ A & im \end{pmatrix}} \right\rangle \quad (21)$$

where averaging is now over rectangular matrices. For our purposes we will need the resolvent calculated at $z = 0$ only. For fixed n_\pm , the result of the averaging over A yields

$$\mathcal{G} = g \mathbf{1} + g_5 \gamma_5 \quad (22)$$

with $\mathcal{G} = \mathcal{G}(0)$ and

$$g = \frac{\frac{i}{2} \left(-m^2 - 2x^2 + m\sqrt{4+m^2+\frac{4x^2}{m^2}} \right)}{m(1-x^2)}$$

$$g_5 = \frac{\frac{i}{2}x \left(m^2 + 2 - m\sqrt{4+m^2+\frac{4x^2}{m^2}} \right)}{m(1-x^2)} \quad (23)$$

and

$$x = \frac{\chi}{2N} = \frac{n_+ - n_-}{2N} \quad (24)$$

Both $\mathbf{1}$ and γ_5 in (22) are $2N \times 2N$ valued. The explicit form of the resolvent g with $m = -iz$ in the chiral limit, can be checked by other methods [24,25]¹. Both g and g_5 are flavor additive. We observe that

$$\text{tr } \mathcal{G} = g + xg_5 = \frac{i}{2} \left(-m + \sqrt{4+m^2+4\frac{x^2}{m^2}} \right) \quad (25)$$

and

$$\text{tr } \gamma_5 \mathcal{G} = xg + g_5 = \frac{ix}{m} \quad (26)$$

For $x = 0$ (square matrices) the discontinuity of (25)

$$\nu_+(\lambda, x=0) = -\frac{1}{\pi} \text{Im } \text{tr } \mathcal{G}(m = -i\lambda + 0) \quad (27)$$

is just Wigner's semicircle for the quark spectral distribution. The argument of \mathcal{G} in (27) has been appended for clarity. For $x \neq 0$ (asymmetric matrices) it is the resolvent in a configuration of unequal topological charges

$$\nu_+(\lambda, x) = |x| \delta(\lambda) + \frac{1}{2\pi|\lambda|} \sqrt{(\lambda^2 - \lambda_-^2)(\lambda_+^2 - \lambda^2)} \quad (28)$$

with $\lambda_{\pm}^2 = 2 \pm 2\sqrt{1-x^2}$. The delta function at the origin, reflects on the number of unpaired topological charges. Configurations with $x \neq 0$ do not break spontaneously chiral symmetry, owing to the occurrence of a gap at the origin. The spontaneous breaking is triggered by the neutral topological configurations with $x = 0$.

We observe that the discontinuity in (26) for fixed x

$$\nu_-(\lambda, x) = -\frac{1}{\pi} \text{Im } \text{tr}(\gamma_5 \mathcal{G})(m = -i\lambda + 0) = x \delta(\lambda) \quad (29)$$

is a direct measurement of the difference in the spectral distribution between left-handed λ_n^- and right handed λ_n^+ quark zero-modes. The result (29) reflects on the Atiyah-Singer index theorem.

In the large N limit, the fluctuations in χ are of order \sqrt{N} , and a statistical averaging over an ensemble of asymmetric matrices yields $x = 0$ on the average. A convenient way of interpreting the averaging over χ diagrammatically is to consider the partition function (13) as describing the interaction of random matrices with a field χ whose propagator is $\langle \chi \chi \rangle = N \chi_*$ (see Fig. 1).

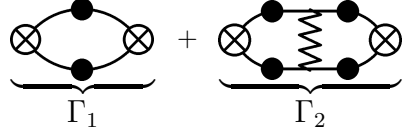


FIG. 2. ‘Trace’ contribution ($\Gamma_1 + \Gamma_2$) to the pseudoscalar susceptibility.

• Gluon Ladder

In the next step we consider the resummation of the gluon ladder. If the resolvent is diagonal²

$$\mathcal{G} = (-i)(a_0 \mathbf{1} \lambda_0 + a_8 \mathbf{1} \lambda_8) \quad (30)$$

and the resummed planar propagator is decomposed as

$$\frac{1}{4N} (D_I^s \otimes (\mathbf{1} \lambda_I) - D_I^{ps} \otimes (\gamma_5 \lambda_I)) \quad (31)$$

in analogy with (20), then the resummation of the rainbow diagrams gives

$$D_I^s = \mathbf{1} \lambda_I + \frac{1}{2} (\text{tr} \lambda_I \mathcal{G} \lambda_J \mathcal{G}) D_J^s \quad (32)$$

$$D_I^{ps} = \gamma_5 \lambda_I - \frac{1}{2} (\text{tr} \lambda_I \mathcal{G} \lambda_J \mathcal{G}) D_J^{ps} \quad (33)$$

This resummation is shown in the form of a Schwinger-Dyson equation in Fig 1. The final result is

$$\mathcal{D}_{\text{resummed}} = \frac{1}{2N} \left(\left[\frac{1}{2+d} \right]_{IJ} \mathbf{1} \lambda_I \otimes \mathbf{1} \lambda_J - \left[\frac{1}{2-d} \right]_{IJ} \gamma_5 \lambda_I \otimes \gamma_5 \lambda_J \right) \quad (34)$$

where d is 9×9 matrix valued

$$d_{IJ} = -\text{tr} \lambda_I \mathcal{G} \lambda_J \mathcal{G} \quad (35)$$

The denominators $2 \pm d$ in the pseudoscalar channel can be interpreted within the effective quark-meson analogy as generalized GMOR (Gell-Mann-Oakes-Renner) relations. Using these results we may now evaluate the pseudoscalar susceptibility.

²Throughout $m_u = m_d \neq m_s$.

¹ Note that a different measure was used in [25].

B. The Puzzle

Now consider the pseudoscalar axial-singlet susceptibility in ChRMM

$$\langle \psi^\dagger \lambda_0 \gamma_5 \psi \psi^\dagger \lambda_0 \gamma_5 \psi \rangle_c \quad (36)$$

Let us first look at the diagrams corresponding to the first line (“trace term”) in (17). The graphs that contribute to the ‘trace’ part are shown in Fig. 2. The “trace-trace” term, corresponding to second line of (17), will be considered later. We remark that main difference between the singlet and nonsinglet pseudoscalar correlators is the second line of (17).

The first graph in Fig. 2 is given by

$$\Gamma_1 = \text{tr } \mathcal{G} \gamma_5 \lambda_0 \mathcal{G} \gamma_5 \lambda_0 = \frac{2}{3} \text{tr } \mathcal{G}^2 \quad (37)$$

The prefactor of $2/3$ follows from our choice of $\lambda_0 = \sqrt{2/3}$. Note that we may safely set $x = 0$ here. The second graph in Fig. 2 is given by

$$\Gamma_2 = \text{tr}(\mathcal{G} \gamma_5 \lambda_0 \mathcal{G}) \mathcal{D}_{\text{resummed}}(\mathcal{G} \gamma_5 \lambda_0 \mathcal{G}) \quad (38)$$

A simpler way to evaluate this graph is to use the identity

Note that the bare “quark lines” carry only a factor 1 (amputated propagators). This identity comes as a result of contracting a bare gluonic propagator (20) with a $\gamma_5 \lambda_0$ vertex. Using the definition of the resummed propagator (Schwinger-Dyson equation) we arrive at the useful identity

Applying the above identity twice, yields

We remark that in the sum $\Gamma_1 + \Gamma_2$ the Γ_1 term cancels against the first one in the above line and the result for the sum is simply the sum of the two remaining diagrams in the line above, that is

$$\begin{aligned} \Gamma_1 + \Gamma_2 &= +4N + (2N \cdot 2) \frac{-1}{2N} \left[\frac{1}{2-d} \right]_{00} (2N \cdot 2) \\ &= 4N \left(1 - 2 \left[\frac{1}{2-d} \right]_{00} \right) \\ &= \frac{-4N}{3} \sum_{i=0}^{N_f} \frac{2}{m_i(\sqrt{4+m_i^2}+m_i)} \end{aligned} \quad (39)$$

The diagrams of Fig. 2 yield a Goldstone pole in the pseudoscalar axial-singlet correlator, hence the *a priori* puzzle.

Before we proceed to solve the puzzle, we note the remarkable cancelation in the sum $\Gamma_1 + \Gamma_2$. The self-energy insertions on the two-quark lines and the one-gluon exchange diagram, conspire to remove the “constituent” quark cut, leading to a Goldstone pole. For the nonsinglet channels this is the mechanism by which the Goldstone modes emerge in a correlation function that does not abide by confinement. This cancelation is reminiscent of the one taking place in two-dimensional QCD in the planar approximation [26]. So it appears that the removal of the “constituent” quark cut is a simple consequence of a consistent treatment of a Ward identity (vertex and self-energy) without the need of confinement.

C. The Solution

In the previous section we have neglected the effects due to the asymmetry in n_\pm as they appear to be subleading in $1/N$, along with the quark loops. In a way, we derived a quenched result. However, the occurrence of strong infrared sensitive terms of the form $x/m \sim 1/\sqrt{N}m$ in the diagrammatic expansion requires that we resum them, prior to taking $N \rightarrow \infty$ for finite m . We show below, that the infrared sensitive terms upset naive power counting in the axial singlet channel. They are just a manifestation of a screening phenomenon in a statistical ensemble made of negative and positive topological charges. Technically the necessity of rederiving $1/N$ counting rules stems from the fact that we have introduced here a non-large N ingredient — the χ field.

The new diagrams that can contribute to our above analysis are the formerly disconnected quark loops which now interact via χ propagators. Looking at a few diagrams we conclude that

- the χ lines cannot end on the same quark loop. This gives a subleading contribution in $1/N$.
- when considering the Green’s function (a 1-point correlator) we get no additional graphs.
- two point correlators of the type

$$\langle \psi^\dagger \Gamma \psi \psi^\dagger \Gamma \psi \rangle \quad (40)$$

get contributions on the endpoints from graphs proportional to x interacting through a dressed χ propagator.

- the dressed χ propagator gets contributions from the part of a closed quark loop which is proportional to x^2 .

With the above observations, we now proceed to solve the puzzle.

D. Screening

Here we isolate the contribution of the closed quark loop Γ which is of order χ^2 . For that consider a general Feynman graph made up of *undressed* quark and gluon propagators. A factor proportional to χ can only appear from a summation in a quark loop (with the γ_5 part of a propagator contributing). Therefore we must have two distinguished quark loops in the graph Γ . Now we may reduce the parts of Γ lying ‘at the edges’ and between the distinguished loops. The former transform into a trace of the (symmetric) Green’s function, while the latter one becomes the resummed gluon propagator (34). We must yet ensure that each loop picks up a factor of χ . For this we must take only the γ_5 channel of the resummed propagator. In the end we obtain:

$$-(-1)\text{tr}(\mathcal{G}\gamma_5\lambda_I) \cdot \frac{1}{2N} \left[\frac{1}{2-d} \right]_{IJ} \text{tr}(\mathcal{G}\gamma_5\lambda_J) \quad (41)$$

The first minus sign comes from the fermion loop, while the second one from the resummed gluon propagator. This gives (recall eq. (30))

$$-\chi^2 c_I \frac{1}{2N} \left[\frac{1}{2-d} \right]_{IJ} c_J \quad (42)$$

with $c_I = i\text{tr} \mathcal{G}\lambda_I$. Resummation gives

$$\chi_{top} = \frac{1}{\frac{1}{\chi_*} + \frac{1}{2}c_I \left[\frac{1}{2-d} \right]_{IJ} c_J} \quad (43)$$

Using the definitions for c_I and d_{IJ} we obtain

$$\frac{1}{\chi_{top}} - \frac{1}{\chi_*} = \sum_{i=1}^{N_f} \frac{1}{m_i \sqrt{4+m_i^2} + m_i^2} \quad (44)$$

For $N_f = 0$ (quenched) the topological susceptibility is $\chi_{top} = \chi_*$, as it should. For $N_f \neq 0$ (unquenched) the topological susceptibility is screened by the quark loops and vanishes in the chiral limit [18]. The alternative, non-diagrammatic proof of equality (44) is presented in Appendix A.

E. Pseudoscalar susceptibility

Given the above observations, we conclude that our previous calculation for Γ_1 and Γ_2 is correct. However our neglect of the term from the second line in (17) is not correct. Although, this term cannot receive a contribution from gluon insertions as they are suppressed in $1/N$, they may have a contribution through a fluctuation in the size of the quark matrices \mathbf{Q} . This is essentially an exchange of a $\chi \sim \sqrt{N}$ field as shown in Fig. 3.



FIG. 3. ‘Trace-trace’ contribution (Γ_3) to the pseudoscalar susceptibility.

The quark loop with $\gamma_5\lambda_0$ insertion gives

$$\text{tr} \mathcal{G}\gamma_5\lambda_0 = 2N \sqrt{\frac{2}{3}} \left(\sum_{j=0}^{N_f} \frac{i}{m_j} x + O(x^2) \right) \quad (45)$$

so the relevant part is just $\sqrt{2/3} \sum_j \frac{i}{m_j} \chi$. The full graph gives

$$\Gamma_3 = -\frac{2}{3} \left(\sum_{i=1}^{N_f} \frac{1}{m_i} \right)^2 \frac{1}{\frac{1}{\chi_*} + \sum_{i=1}^{N_f} \frac{1}{m_i(\sqrt{4+m_i^2} + m_i)}} \quad (46)$$

The susceptibility is then the sum of the two graphs of Fig. 2 and the graph of Fig. 3, that is

$$\Gamma_1 + \Gamma_2 - \Gamma_3 = \frac{2N}{3} \left[\left(\sum \frac{1}{m_i} \right)^2 \frac{1}{\frac{1}{\chi_*} + \sum S_i} - 4 \sum_i S_i \right] \quad (47)$$

where we used the notation

$$S_i = \frac{1}{m_i(\sqrt{4+m_i^2} + m_i)} \quad (48)$$

For equal quark masses we get

$$\begin{aligned} \chi_{ps} &= -\frac{2N}{3} \left[-12S + \frac{9/m^2}{\frac{1}{\chi_*} + 3S} \right] \\ &= -\frac{2N}{3} \frac{\frac{9}{m^2} - \frac{12S}{\chi_*} - 4 \cdot 9S^2}{\frac{1}{\chi_*} + 3S} \end{aligned} \quad (49)$$

Since our choice of $\lambda_0 = \sqrt{2/3}$ and γ_5 is $2N \times 2N$ valued with $n_+ + n_- = 2N$ fixed, the prefactor of $2N/3$ is natural in (49). The properly normalized susceptibility is

$$\tilde{\chi}_{ps} = \frac{3}{2N} \chi_{ps} = \frac{3}{2N} (\Gamma_3 - \Gamma_1 - \Gamma_2) \quad (50)$$

which is finite in the large N limit.

In the chiral limit $S \sim 1/2m$ and the leading singularities in $1/m^2$ cancel in the numerator. The pseudoscalar susceptibility χ_{ps} is finite in the chiral limit, thereby solving the $U(1)$ problem. The *a priori* Goldstone pole in $\Gamma_1 + \Gamma_2$ was removed (screened) by the order \sqrt{N} fluctuations in the size of the matrices. Although our result was derived with a gaussian weight in A , we believe the latter to be a fixed point as discussed in [27].

F. Scalar Susceptibility

Similar arguments for the scalar susceptibility

$$\chi_s = \frac{1}{V_4} \int d^4x \langle T^* \bar{\psi} \psi(x) \bar{\psi} \psi(0) \rangle_c \quad (51)$$

translates in ChRMM to

$$\begin{aligned}\chi_s &= \frac{1}{N} [-\langle \text{tr} \mathbf{Q}^{-1} \mathbf{Q}^{-1} \rangle] \\ &+ \frac{1}{N} [\langle \text{tr}(\mathbf{Q}^{-1}) \text{tr}(\mathbf{Q}^{-1}) \rangle_c]\end{aligned}\quad (52)$$

ignoring (ultraviolet sensitive) contributions from continuum states. Similar correlators using also results from random matrix theory where also discussed in [28].

Since the scalar susceptibility is proportional to the derivative of the Green's function with respect to the mass, we can immediately write down the result for (52) in the form

$$\chi_s = N_f \left(1 - \frac{m}{\sqrt{4+m^2}} \right) \quad (53)$$

This result is only qualitative, since we have ignored the effects of the scale anomaly. Also for small values of m , (53) does not show terms of the form $\ln m$ expected from the exchange of two Goldstone modes. In ChRMM these exchanges are $1/N$ suppressed.

G. Numerical Results

To check on the validity of the above arguments, we have carried out direct numerical calculations using a gaussian distributed ensemble of rectangular matrices. Figures 4 and 5 show the results of the numerical simulations for the topological, pseudoscalar and scalar susceptibilities, with one and three flavors respectively. The solid lines follow from (44), (49), and (53) respectively. Our $1/N$ analysis is confirmed, except for very small values of m , where finite $1/N$ size effects are noted. Throughout χ_* was set to 1.

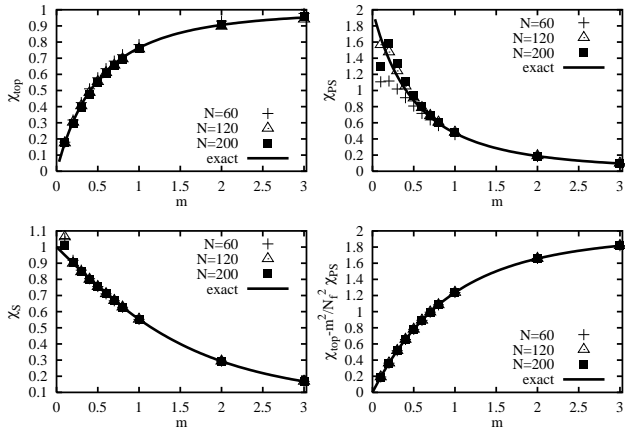


FIG. 4. Normalized topological (upper left), pseudoscalar (upper right), scalar (lower left) susceptibilities, and Ward identity (lower right) for $N_f = 1$. The numerical simulations were carried for fixed $2N = n_+ + n_- = 60, 120, 200$ and $\langle (n_+ - n_-)^2 \rangle = N\chi_* = N$. The solid line is our analytical result.

We have checked that our numerical results are in agreement with the Ward identity (6) when translated to ChRMM. Specifically

$$\chi_{top} + \frac{m^2}{N_f^2} \tilde{\chi}_{ps} = -\frac{2mi}{N_f^2} \text{tr} \mathcal{G} \quad (54)$$

The proof of the above identity is included in Appendix B. Figures 4 and 5 (lower right) show the Ward identity (54). The numerical points represent the l.h.s. of the Ward identity, the solid line is calculated from the analytical prediction for the r.h.s. using (25) with $x = 0$.

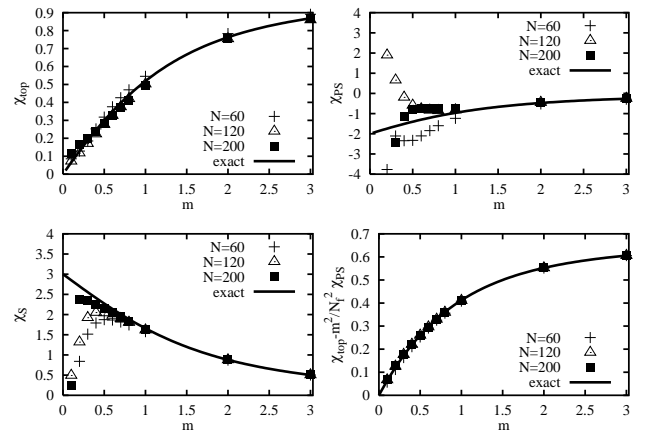


FIG. 5. Same as Fig. 4 but for $N_f = 3$.

V. CONCLUSIONS

We have shown that an ensemble of asymmetric but standard ChRMM with an assumed gaussian distribution for the asymmetry, yields a screened topological susceptibility and solves the $U(1)$ problem. We believe this result to be new in the context of ChRMM. Using diagrammatic techniques in the context of the $1/N$ approximation, we have shown the fermion determinant contributes importantly in the axial-singlet channel through infrared sensitive terms, but otherwise is quenched in most other channels in the thermodynamical limit. We also believe that this result is new in the context of ChRMM. Some of these results are generic and illustrative of the mechanisms at work in more realistic models of the QCD vacuum, such as the instanton liquid model. It would be interesting to see how the present arguments extend to nonstandard ChRMM [29], and how they are modified at high temperature and finite N in comparison to current lattice simulations [30]. Also, our analysis allows for an assessment of the θ vacua in ChRMM, as we will discuss next.

Acknowledgments

This work was supported in part by the US DOE grant DE-FG-88ER40388, by the NSF grant NSF-PHY-94-

21309, by the Polish Government Project (KBN) grants 2P03B19609, 2P03B08308 and by the Hungarian Research Foundation OTKA. One of us (R.A.J) thanks the Nuclear Theory Group in Stony Brook and GSI for their hospitality.

Appendices

A. Screened Topological Susceptibility

In this Appendix, we will outline an alternative derivation in favor of the screening of the topological charge in the present model. The connected ‘vacuum’ diagrams (prior to averaging over χ) are given by $\log Z(\chi)$. For a fixed asymmetry $x = \chi/2N = (n_+ - n_-)/2N$ we have

$$\begin{aligned} \partial_m \log Z(\chi) &= -i\langle\psi^\dagger\psi\rangle = -2Ni\text{tr}\mathcal{G} \\ &= NN_f \left(-m + \sqrt{4+m^2 + \frac{4x^2}{m^2}} \right) \end{aligned} \quad (55)$$

The contribution of order x^2 follows by expanding the right hand side

$$(\partial_m \log Z(\chi))_2 = NN_f \frac{2x^2}{m^2\sqrt{4+m^2}} \quad (56)$$

and integrate it with respect to m to obtain

$$(\log Z(\chi))_2 = NN_f \left(-\frac{\sqrt{m^2+4}}{2m} + \text{const} \right) x^2 \quad (57)$$

The constant is set by the requirement that for $m \rightarrow \infty$ we should obtain zero. Hence

$$(\log Z(\chi))_2 = NN_f \left(-\frac{\sqrt{m^2+4}}{2m} + \frac{1}{2} \right) \cdot x^2 = \quad (58)$$

$$= -2NN_f \frac{1}{m(\sqrt{4+m^2}+m)} \cdot x^2 \quad (59)$$

$$= -\frac{1}{2N} N_f \frac{1}{m(\sqrt{4+m^2}+m)} \cdot \chi^2 \quad (60)$$

The full partition function is given by

$$Z = \int d\chi e^{-\frac{\chi^2}{2\chi_* N}} Z(\chi). \quad (61)$$

Inserting (60) into (61) yields

$$Z = \int d\chi e^{-\frac{1}{2N} \left(\frac{1}{\chi_*} + N_f \frac{1}{m(\sqrt{4+m^2}+m)} \right) \chi^2 + \dots} \quad (62)$$

in agreement with (44).

B. Ward identity in ChRMM

The Ward identity (54) can be derived from the partition function for finite θ angle and massive quarks. Specifically

$$Z[\theta] = \langle \det^{N_f} \begin{pmatrix} im e^{i\frac{\theta}{N_f}} & A^\dagger \\ A & im e^{-i\frac{\theta}{N_f}} \end{pmatrix} \rangle = \langle \det^{N_f} \mathbf{Q}_\theta \rangle \quad (63)$$

Using the derivatives at $\theta = 0$

$$\partial_\theta \mathbf{Q}_\theta = -\frac{m}{N_f} \gamma_5 \quad (64)$$

and

$$\partial_\theta^2 \mathbf{Q}_\theta = -\frac{im}{N_f^2} \mathbf{1} \quad (65)$$

we get

$$N\chi_{top} = \frac{-im}{N_f^2} \langle\psi^\dagger\psi\rangle - \frac{m^2}{N_f^2} \langle\psi^\dagger\gamma_5\psi\psi^\dagger\gamma_5\psi\rangle \quad (66)$$

Since $\langle\psi^\dagger\psi\rangle = 2N\text{tr}\mathcal{G}$, then

$$\chi_{top} = -\frac{2m}{N_f^2} i\text{tr}\mathcal{G} - \frac{m^2}{N_f^2} \tilde{\chi}_{ps} \quad (67)$$

in agreement with (54).

-
- [1] H. Fukuda, *et al*, Prog. Theor. Phys. **4** (1949) 477; S.L. Adler, Phys. Rev. **177** (1969) 2426; J.S. Bell and R. Jackiw, Nuov. Cim. **60 A** (1969) 47.
 - [2] G. 't Hooft, Phys. Rev. Lett. **37** (1976) 8; Phys. Rep. **142** (1986) 357.
 - [3] E. Witten, Nucl. Phys. **B156** (1979) 269; Ann. Phys. **128** (1980) 363.
 - [4] G. Veneziano, Nucl. Phys. **B159** (1979) 269.
 - [5] M. Teper, Nucl. Phys. [Suppl.] **B20** (1991) 159; A. Di Giacomo, Nucl. Phys. [Suppl.] **B23** (1991) 191.
 - [6] K.M. Bitar, *et al*. Phys. Rev. **D44** (1991) 2090; Y. Kurokoshi, *et al*. Phys. Lett. **B313** (1993) 425.
 - [7] H. Yamagishi and I. Zahed, “BRST Quantization, Strong CP Violation, the U(1) problem, and θ Vacua”, e-print : hep-ph/9507296.
 - [8] S. Samuel, Mod. Phys. Lett. **37** (1992) 2007; H. Kikuchi and J. Wudka, Phys. Lett. **284** (1992) 111; N. Dowrick and M.C. McDougall, Phys. Lett. **B285** (1992) 269.
 - [9] E.V. Shuryak and J.J.M. Verbaarschot, Nucl. Phys. **A560** (1993) 306; J.J.M. Verbaarschot and I. Zahed, Phys. Rev. Lett. **70** (1993) 3852; For an early account see : M.A. Nowak, J.J.M. Verbaarschot and I. Zahed, Phys. Lett. **B217** (1989) 157; Yu. A. Simonov, Phys. Rev. **D43** (1991) 3534.
 - [10] M.A. Halasz and J.J.M. Verbaarschot, Phys. Rev. Lett. **74** (1995) 3920; J.J.M. Verbaarschot, “Random Matrix Model Approach to Chiral Symmetry”, e-print: hep-lat/9607086.

- [11] M. Stephanov, Phys. Lett. **B375** (1996) 249; T. Wettig, A. Schäfer and H.A. Weidenmüller, Phys. Lett. **B367** (1996) 28.
- [12] J. Jurkiewicz, M.A. Nowak and I. Zahed, “ Dirac Spectrum in QCD and Quark Masses”, e-print: hep-ph/9604235, Nucl. Phys. **B** (in Print); M.A. Nowak, G. Papp and I. Zahed, “QCD-inspired Spectra from Blue’s Functions”, e-print: hep-ph/9603348, Phys. Lett. **B** (in Print).
- [13] T. Schäfer and E.V. Shuryak, “Instantons in QCD”, e-print : hep-ph/9610451, and references therein.
- [14] D. Diakonov, “Chiral Symmetry Breaking by Instantons”, e-print : hep-ph/9602375, and references therein.
- [15] M.A. Nowak, M. Rho and I. Zahed, “Chiral Nuclear Dynamics”, World Scientific 1996, and references therein.
- [16] R.A. Janik, M.A. Nowak, G. Papp and I. Zahed, “Macroscopic Universality: Why QCD in Matter is Subtle?”, e-print: hep-ph/9606329, Phys. Rev. Lett. (in Print).
- [17] R.J. Crewther, in Field Theoretical Methods in Particle Physics, edited by W. Ruhl, Plenum N.Y. 1980; G.A. Christos, Phys. Rep. **116** (1984) 251.
- [18] M.A. Shifman, A.I. Vainshtein and V.I. Zakharov, Nucl. Phys. **B166** (1980) 439; D.I. Diakonov and M.I. Eides, Sov. Phys. JETP **54** (1981) 232.
- [19] M.A. Nowak, J.J.M. Verbaarschot and I. Zahed, Phys. Lett. **B228** (1989) 251; R. Alkofer, M.A. Nowak, J.J.M. Verbaarschot and I. Zahed, Phys. Lett. **B233** (1989) 205; M. Kacir, M. Prakash and I. Zahed, “Hadrons and QCD instantons: A bosonized view”, hep-ph/9602314.
- [20] C. Rozenzweig, J. Schechter and G. Trahern, Phys. Rev. **D21** (1980) 3388; P. Di Vecchia and G. Veneziano, Nucl. Phys. **B171** (1980) 253; E. Witten, Ann. Phys. **128** (1981) 1789; P. Nath and R. Arnowitt, Phys. Rev. **D23** (1981) 473.
- [21] I. Zahed, Nucl. Phys. **B427** (1994) 561; J.J.M. Verbaarschot and E.V. Shuryak, Phys. Rev. **D52** (1995) 295.
- [22] D.I. Diakonov, M.V. Polyakov and C. Weiss, “Hadronic matrix elements of gluon operators in the instanton vacuum”, hep-ph/9510232.
- [23] M.A. Shifman, Phys. Rep. **209** (1991) 341.
- [24] R.A. Janik, M.A. Nowak, G. Papp, J. Wambach and I. Zahed, “Nonhermitean Random Matrix Models: A Free Random Variable Approach”, hep-ph/9609491.
- [25] J. Feinberg and A. Zee, “Renormalizing Rectangles and Other Topics in Random matrix Theory”, cond-mat/9609190.
- [26] G. ’t Hooft, Nucl. Phys. **B75** (1974) 461.
- [27] E. Brézin and A. Zee, Nucl. Phys. **B402** (1993) 613.
- [28] M.A. Nowak, J.J.M. Verbaarschot and I. Zahed, Nucl. Phys. **B324** (1989) 1; M.A. Nowak, J.J.M. Verbaarschot and I. Zahed, Phys. Lett. **B217** (1989) 157.
- [29] R.A. Janik, M.A. Nowak and I. Zahed, “Chiral Random Matrix Models: Thermodynamics, Phase Transitions and Universality”, Phys. Lett. **B** (in Print).
- [30] C. Bernard, *et al.*, “Thermodynamics for Two Flavor QCD”, e-print : hep-lat/9608026; J.B. Kogut, J.-F Lagaë and D.K. Sinclair, “Manifestation of the Axial Anomaly in Finite Temperature QCD”, e-print : hep-lat/9608128.